Journal of Adhesion Science and Technology

ISSN: 0169-4243 (Print) 1568-5616 (Online) Journal homepage: https://www.tandfonline.com/loi/tast20

Ultrasonic detection of kissing bonds at adhesive interfaces

Peter B. Nagy

To cite this article: Peter B. Nagy (1991) Ultrasonic detection of kissing bonds at adhesive interfaces, Journal of Adhesion Science and Technology, 5:8, 619-630, DOI: 10.1163/156856191X00521

To link to this article: https://doi.org/10.1163/156856191X00521

J. Adhesion Sci. Technol. Vol. 5, No. 8, pp. 619–630 (1991)

Ultrasonic detection of kissing bonds at adhesive interfaces

PETER B. NAGY

Department of Welding Engineering, The Ohio State University, 190 W. 19th Avenue, Columbus, OH 43210, USA

Revised version received 17 May 1991

Abstract—Intimate mechanical contact between the adhesive and adherend counterparts can easily occur without an actual bond. Such apparently flawless, but severely defective 'kissing' bonds are especially dangerous because they often remain hidden from most types of conventional ultrasonic inspection. A special high-frequency, high-inspection angle ultrasonic technique is suggested to improve the detectability of such kissing bonds. It is shown to be essential to interrogate the adhesive–adherend interface from the adherend side without sending the ultrasound through the inherently inhomogeneous and highly attenuating adhesive layer.

Keywords: Adhesive bond; interface evaluation; ultrasound.

1. INTRODUCTION

A kissing bond occurs as a result of plastic contact between smooth or slightly rough surfaces. It is a typical interfacial defect, i.e. the cohesive properties of the adhesive material are not affected at all. A kissing bond produces very low contrast in ultrasonic inspection since there is an intimate mechanical contact between the counterparts without an actual bond. Besides some weak sticking effects, such a 'bond' has practically no strength at all. When a kissing bond occurs in localized spots surrounded by more-or-less well-bonded areas, sufficient compressive residual stress might persist at the defective interface to hide it from low-level ultrasonic nondestructive evaluation (NDE) until it is turned into an actual delamination by excessive load.

In order to study the interaction of ultrasonic waves with kissing-bonded adhesive interfaces, we should consider 'thin' imperfections only when the overall thickness of the affected interface region is negligible with respect to the wavelength of the ultrasonic wave used to inspect the boundary. Such essentially two-dimensional interfaces can be easily modeled by the well-known finite boundary stiffness technique. Figure 1 shows the geometrical configuration of the interface problem. The boundary conditions require that both tangential (T_{xy}) and normal (T_{yy}) components of the stress must be continuous at the interface, but there is a local discontinuity of the displacement components. The resulting displacement jump through the interface is proportional to the corresponding stress components:

$$T_{yy}^{A} = T_{yy}^{B} = S_{L}(u_{y}^{B} - u_{y}^{A}) \tag{1}$$

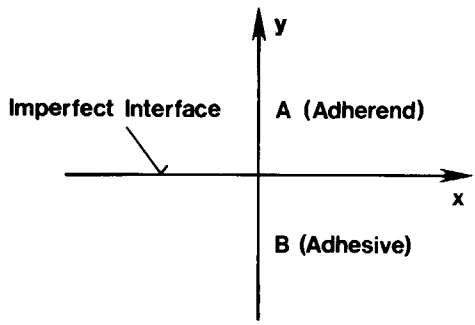

Figure 1. Coordinate system for the adhesive interface.

and

$$T_{xy}^{A} = T_{xy}^{B} = S_T(u_x^B - u_x^A), \tag{2}$$

where u_x and u_y denote the transverse and normal displacements, and S_L and S_T are the extensional and transverse interfacial stiffness constants of the imperfect interface (superscripts A and B indicate the two different sides of the interface) [1–9].

The reflection and transmission coefficients $R_{L,T}$ and $T_{L,T}$ of such an interface can be calculated from equations (1) and (2) for any combination of longitudinal and transverse waves at arbitrary incidence [3, 7, 9]. For the simplest case of normal incidence, the following well-known results can be obtained:

$$R_{L,T} = \frac{R'_{L,T} + \dfrac{i\omega}{\Omega_{L,T}}}{1 + \dfrac{i\omega}{\Omega_{L,T}}} \tag{3}$$

$$T_{L,T} = \frac{T'_{L,T}}{1 + \dfrac{i\omega}{\Omega_{L,T}}}, \tag{4}$$

where subscripts L and T correspond to longitudinal and transverse waves, respectively [both equations (3) and (4) correspond to two separate equations]; the prime indicates the corresponding reflection and transmission coefficients of the ideal adherend–adhesive interface; ω denotes the angular frequency; and Ω_L and Ω_T are the characteristic transition frequencies between the low-frequency and high-frequency regions.

Figure 2 shows these reflection and transmission coefficients as a function of the frequency. At very low frequencies, the interface appears to be perfect. As the frequency increases, the reflection increases to 100% while the transmission drops to zero. The characteristic frequency (Ω), where the transition from the apparently perfect interface to the apparently delaminated one occurs, is somewhat different for longitudinal and transverse incidence. Actually, the ratio of

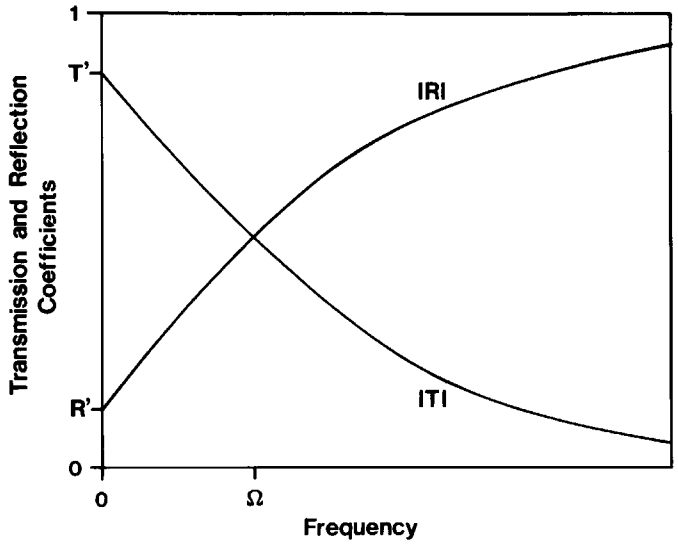

Figure 2. Reflection and transmission coefficients of an imperfect interface as a function of the frequency at normal incidence.

these frequencies (Ω_T/Ω_L) can be shown to be closely related to the physical nature of the interface imperfection and, therefore, plays a very important role in the evaluation of the measured ultrasonic signals.

2. DIFFERENT TYPES OF IMPERFECTIONS

The finite boundary stiffness approximation of equations (1) and (2) can be used to model imperfect interfaces of very different physical natures, e.g. partial bond, kissing bond, slip bond, etc. A partial bond consists of a number of unbonded areas in the interface plane which are not resolved individually by the interrogating ultrasonic beam. The overall effect of such an array of cracks on ultrasonic transmission and reflection can be used to measure certain statistical properties of the partial bond [4–7, 9–12], and the measured characteristic frequencies can be easily related to the interface stiffnesses:

$$\Omega_{L,T} = \frac{2S_{L,T}}{c_{L,T}\rho}, \tag{5}$$

where c_L and c_T are the longitudinal and transverse velocities, and ρ denotes the density of the material. For certain simple partial bond patterns, the stiffness constants can be obtained using the deformation results tabulated by Tada *et al.* [13]. For a periodic array of cracks running parallel or normal to the polarization of the transverse wave [6, 9],

$$S_{TP} = (1 - \nu)S_L \tag{6}$$

and

$$S_{TN} = S_L, \tag{7}$$

where ν is the Poisson ratio. For the more realistic model of periodic distribution

of circular cracks, the exact solution is not available. Assuming a constant proportionality connecting S_L with $S_{TP}=S_{TN}$, Margetan *et al.* [9] obtained the following approximate formula from equations (6) and (7):

$$S_T \approx \frac{2-\nu}{2} S_L. \tag{8}$$

The sought-after ratio between the transverse and longitudinal characteristic frequencies can be calculated from equations (5) and (8):

$$\Omega_T/\Omega_L = (S_T/S_L)(c_L/c_T) \approx \frac{2-\nu}{2}\sqrt{\frac{2(1-\nu)}{1-2\nu}}. \tag{9}$$

For most structural materials, ν varies between 0.3 and 0.33 and Ω_T/Ω_L changes from 2.24 to 1.65. In other words, at any frequency a partial bond exhibits a stronger reflection coefficient by longitudinal inspection simply because Ω_T is considerably higher than Ω_L.

An even more dangerous type of interface imperfection, a so-called kissing bond, can occur as a result of plastic contact between smooth or slightly rough surfaces. Besides some very weak 'sticking' effects, a kissing bond practically has no strength, but because of the intimate mechanical contact between the contacting parts, it produces very low ultrasonic contrast, i.e. low reflection and high transmission.

Figure 3 shows a schematic diagram of plastic contact between flat, slightly rough surfaces. The initial contact area comprises a number of isolated islands at the highest points above the mean planes of the rough surfaces. Upon applying a compressive stress (s), the apparent contact area increases via plastic flow in the softer material. Since the mean separation is usually negligible with respect to the

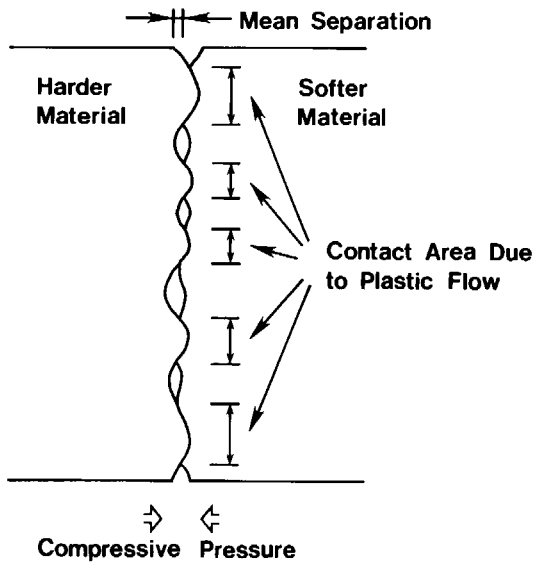

Figure 3. Plastic contact between flat, rough surfaces.

wavelength of the inspecting ultrasound, this essentially two-dimensional interface can be easily modeled by the well-known finite boundary stiffness technique.

S_L and S_T can be determined from the compressive pressure-to-flow pressure ratio (s/p_m) and other parameters, such as surface roughness and elastic moduli, by using Haines's technique [14]. It can be shown that an s/p_m ratio of 10–50% is necessary to achieve good ultrasonic contact of high transmission and low reflection. In most structural materials, the flow pressure (p_m) is of the order of 10^8 N/m^2; therefore, a similar, very high compressive pressure is needed to produce a kissing bond, which is called dry contact in this case. In certain solid-state bonds where the interface is formed as a combined effect of compressive pressure and elevated temperature, e.g. in an inertia friction weld, a diffusion bond, a resistance spot weld, etc., a kissing bond can be produced at much lower pressures around 10^7 N/m^2 because of the greatly reduced flow pressure at high temperatures [15]. Similarly, kissing bonds can be formed at as low as a 10^6 N/m^2 or less in adhesive bonds because of the viscous fluid nature of the uncured adhesive.

Haines found that such a kissing bond can also be modeled by the finite boundary stiffness assumption, and the ratio of the characteristic frequencies can be approximated by

$$\Omega_T/\Omega_L = (G/E)(c_L/c_T) = \frac{1}{2(1+\nu)}\sqrt{\frac{2(1-\nu)}{1-2\nu}}, \tag{10}$$

where E and G are the Young and shear moduli, respectively [14]. In this case, when ν varies between 0.3 and 0.33, Ω_L/Ω_T changes from 0.72 to 0.75. In other words, at any frequency, a kissing bond exhibits a stronger reflection coefficient by shear inspection simply because Ω_T is lower than Ω_L.

Another often applied interface model is the so-called viscous slip condition, which is particularly useful in connection with partially polymerized adhesive bonds [5, 8, 16]. Schoenberg [3] showed that the finite boundary stiffness approach leads to reflection and transmission coefficients of the form of equations (1) and (2). Assuming that the acoustic impedance of the layer is much smaller than that of the bonded half-spaces and that the layer thickness is negligible with respect to the wavelength, the boundary stiffness constants can be calculated as follows:

$$S_L = \frac{B' + (4/3)\mu'}{h} \tag{11}$$

and

$$S_T = \mu'/h, \tag{12}$$

where h is the layer thickness and μ' and B' are the rigidity and bulk modulus of the viscous layer. Substantial transverse slip occurs when the thickness of the hydrodynamic boundary layer $(\eta/\omega)^{1/2}$ is much smaller than the thickness of the interface layer h, and the ultrasonic frequency is low with respect to the shear relaxation time of the fluid. Then

$$\mu' \approx i\omega\eta\rho', \tag{13}$$

where η is the kinematic viscosity of the layer and ρ' is the fluid density, and

$$S_T/S_L \approx \frac{i\omega\eta\rho'}{B'} = \frac{i\omega\eta}{c'^2}, \tag{14}$$

where c' is the compressional wave velocity in the fluid. For ordinary water at 15°C, the kinematic viscosity $\eta \approx 10^{-6}$ m^2/s, $c' \approx 1500$ m/s, and S_T/S_L is as low as 3×10^{-5} at 10 MHz, i.e. almost pure transverse slip occurs. Other couplant materials, such as oil or glycerin, have a much higher viscosity around $\eta \approx 2\times10^{-3}$ m^2/s and S_T/S_L is approximately 5%, while commercial ultrasonic couplants feature a high viscosity of 4×10^{-2} m^2/s or more and S_T/S_L is about 1. We can conclude that a typical viscous slip corresponds to $\Omega_T/\Omega_L \leq 0.1$, i.e. shear wave inspection yields at least ten times higher interface reflection at normal incidence than longitudinal one.

Figure 4 summarizes the above results by showing the shear wave reflection coefficients (solid lines) of different boundary imperfections resulting in identical longitudinal wave reflection (dashed line). A partial bond usually has reduced, but still substantial strength, while a kissing or slip bond has no strength at all. In order to evaluate the measured reflection coefficient in terms of interface properties, we must distinguish between these different imperfections. While a single, either longitudinal or shear, measurement cannot facilitate such identification, the ratio of the characteristic frequencies can do it. Compared with a partial bond, a kissing bond is offset toward the slip boundary case, but a 'strong' kissing bond still represents almost rigid boundary conditions; therefore, it is very difficult to detect.

In order to demonstrate this important property of kissing bonds, Figs 5 and 6 show the shear and longitudinal reflection coefficients of an unbonded interface between compressed aluminum parts. Because of the somewhat random nature of the interface contact, the measurement was repeated ten times and averaged at each stress level. The surfaces were dry, flat, and fairly smooth with less than 0.5 μm rms roughness. These measurements were made at normal incidence by contact transducers; therefore, the shear reflection coefficient depends on the transverse interface stiffness only, while the longitudinal one depends on the

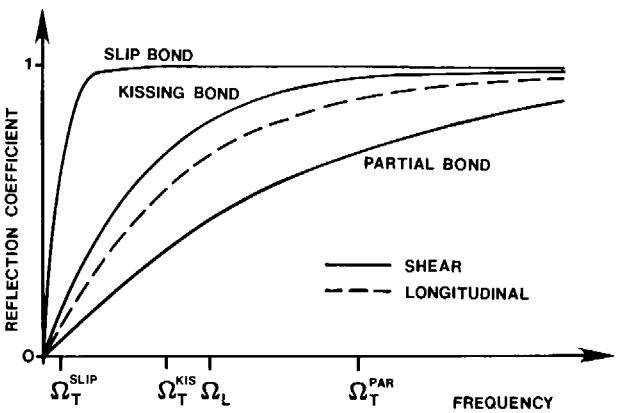

Figure 4. Comparison of different boundary imperfections with identical longitudinal wave reflection.

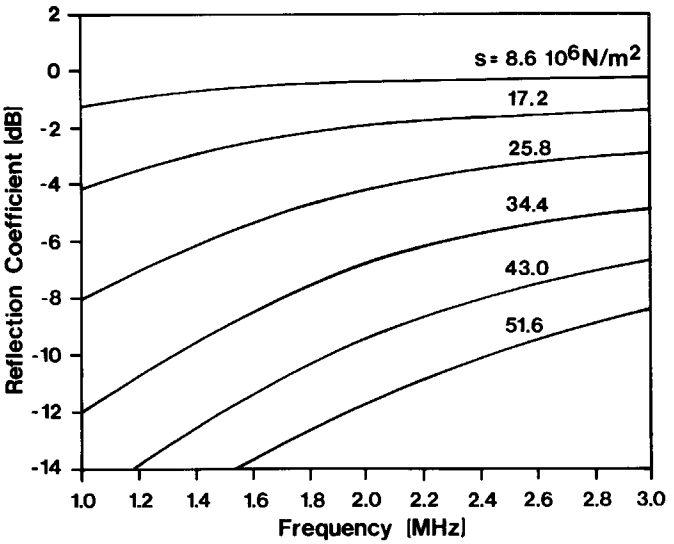

Figure 5. Shear wave reflection at normal incidence from a kissing-bonded aluminum interface at different compressive pressures.

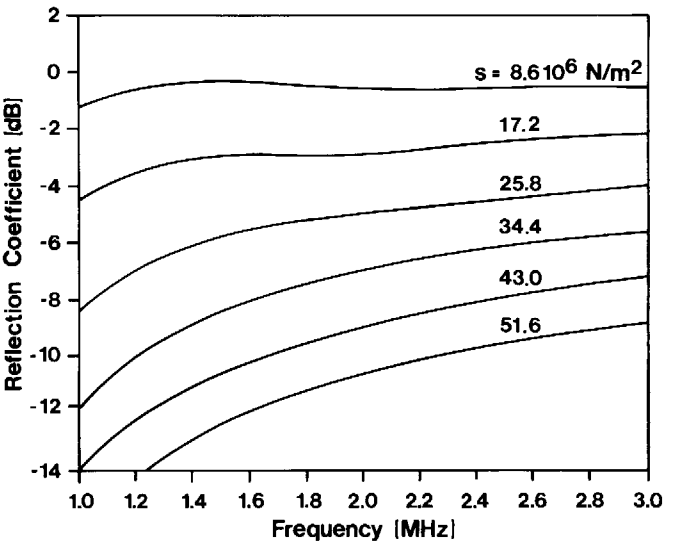

Figure 6. Longitudinal wave reflection at normal incidence from a kissing-bonded aluminum interface at different compressive pressures.

extensional interface stiffness. In good agreement with our expectations, this boundary looks apparently perfect at very low frequencies, but completely delaminated at very high frequencies. The transition frequency shifts upward from ~0.5 MHz to ~8 MHz with increasing compressive pressure and the Ω_T/Ω_L ratio is slightly less than 1. Although there is considerable scatter in the data caused by the somewhat random behavior of the intimate contact produced between the slightly rough counterparts, the average ratio was found to be approximately 0.9, which is also in good agreement with our expectations.

The main conclusion that one can draw from these results is that a kissing bond definitely cannot be simply modeled as a transverse slip. This conclusion will be further verified later by demonstrating that transverse slip produces irreversible damage to the usually very intimate mechanical contact between the adhesive and the adherend, which cannot be re-established once again by eliminating the load.

3. INSPECTION TECHNIQUE

A schematic diagram of the microscopic inspection technique is shown in Fig. 7 [17]. It is called 'microscopic' because of the high-frequency, very sharply focused transducer used in this otherwise conventional C-scan configuration. The necessity of this special arrangement is demonstrated by Fig. 8, showing the shear wave reflection coefficient of an imperfect adherend–adhesive interface as a function of the incident angle for five different frequencies (typical values of Ω_T are between 10 and 100 MHz). As a general rule, the interface appears to be

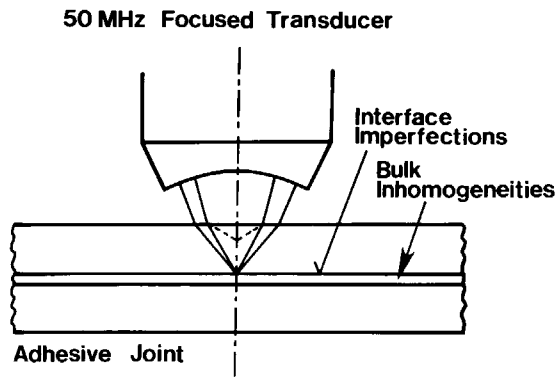

Figure 7. Schematic diagram of the 'microscopic' inspection technique.

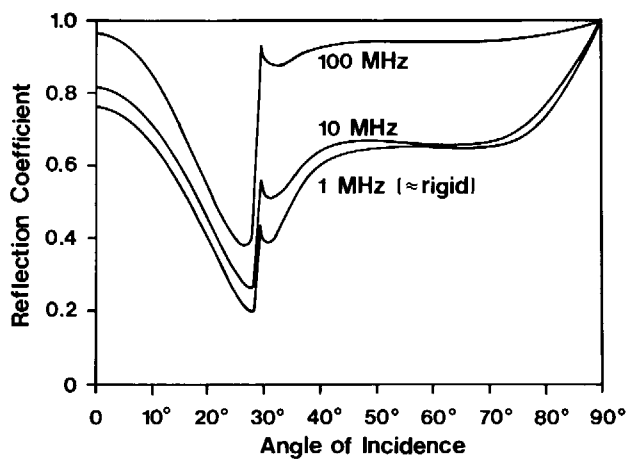

Figure 8. Shear wave reflection coefficient from an imperfect aluminum–adhesive interface ($S_L = 5 \times 10^8$ N/m^3 and $S_T = 10^8$ N/m^3).

'rigid' at very low frequencies. As the frequency increases, the reflection increases to 100% while the transmission drops to zero; therefore, the highest feasible inspection frequency should always be used.

It is well known that a perfect slip ($S_T = 0$) or viscous slip ($S_T \ll S_L$) boundary can be detected much better by producing transverse vibrations at the interface instead of normal ones. Although a kissing bond cannot be modeled adequately by slip boundary conditions, it exhibits a somewhat similar behavior as long as the S_T/S_L ratio is considerably lower than that for other types of imperfections, such as a partial bond. At normal incidence, longitudinal waves are less sensitive while shear waves are difficult to generate. When the transducer is focused below the top surface of the upper adherend plate, there will be two separate focal depths, one for the longitudinal waves and one for the shear ones. In this particular case, we focused the shear components onto the adherend–adhesive interface.

Because of the very high frequency and viewing angle used to inspect the adhesive bondline, this technique is limited to one-sided access only. First, the rather weak interface inhomogeneity, caused by a weak kissing bond, is barely detectable from the fairly homogeneous adherend side, and it would be almost impossible to detect from the inherently inhomogeneous adhesive side where additional scattering from scrim fibers, micro-porosity, etc. usually produces a rather uneven background. Furthermore, because of the inherently high attenuation in most adhesives, we could not go through this layer at such a high frequency even if we wanted to.

4. EXPERIMENTAL RESULTS

Six specimens were prepared to test the sensitivity of the suggested ultrasonic technique. 150 mm × 150 mm, 6 mm-thick Al 2024 plates were bonded by FM300K epoxy adhesive applied as a 150 μm thick layer. The adherend surfaces were treated by BR-127 primer according to the manufacturer's specifications (American Cyanamid Co.). In order to generate localized kissing bonds, five circular spots of 25 mm diameter were painted with a release agent. The locations of these defective areas are shown in Fig. 9. Subsequent destructive (tensile–shear) tests confirmed the actual unbond at the exact locations of the designed kissing bond areas.

Figure 10 shows a typical microscopic C-scan taken from the defective side of the adhesive bond. There are clear indications of increased reflection at each of the five kissing-bonded spots. Figure 11 shows the microscopic C-scan of the same sample from the other side. There is no trace of any defects in this picture, which is expected from such a high-frequency, high-angle inspection.

It is well known that kissing bonds can be easily turned into actual delaminations by applying a sufficient load to separate the unbonded surfaces. This is an irreversible process, i.e. the initial intimate contact will not be re-established after the load is terminated. Figure 12 shows the microscopic C-scan of the same sample taken after a modest deformation of the joint, well within the elastic region. Approximately 1000 N bending force was applied to the center of the 150 mm × 150 mm sample supported at the corners. The resulting, mostly shear stress caused almost complete delamination at three spots and partial

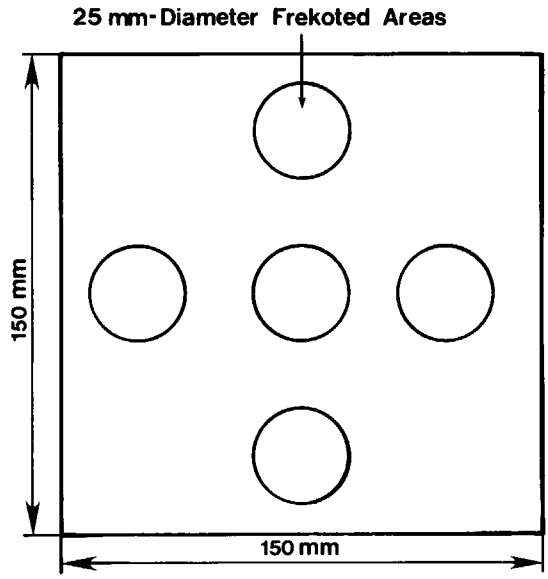

Figure 9. Designed defect locations in the sample, made by applying Frekote 44 release agent.

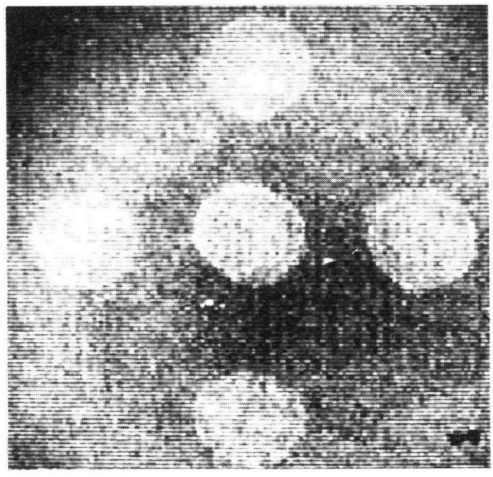

Figure 10. Kissing bonds detected by high-angle inspection at 50 MHz from the defective side.

delamination at one spot out of five. It should be mentioned that these delaminations are readily detectable even on the 10 MHz conventional C-scan shown in Fig. 13. It is also interesting that the inherently one-sided microscopic technique could not detect even these gross defects from the other side of the adhesive joint.

5. CONCLUSIONS

It was shown that kissing bonds usually remain hidden from conventional ultrasonic flaw detection. It was also shown that a kissing-bonded imperfect interface produces slightly higher acoustic contrast for transverse vibrations than

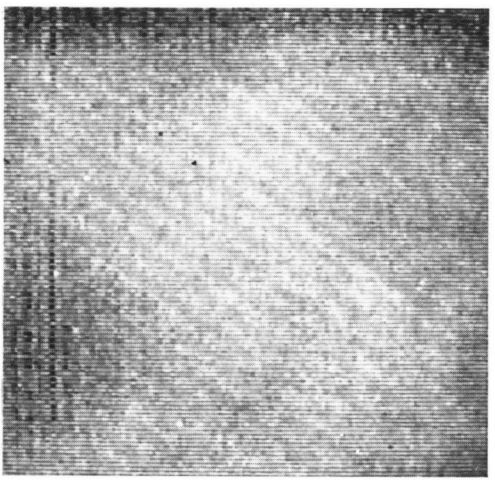

Figure 11. Kissing bonds detected by high-angle inspection at 50 MHz from the other side (see Fig. 10).

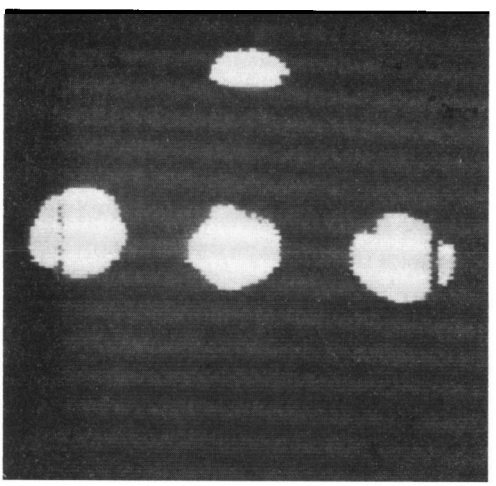

Figure 12. Kissing bonds detected by high-angle inspection at 50 MHz from the defective side after bending.

for longitudinal ones, but it definitely cannot be modeled simply as a slip boundary. Although the better sensitivity of shear wave inspection has been previously observed experimentally, its origin in the particular physical nature of the kissing contact has not been clearly understood. A high-frequency, high-angle inspection technique was suggested to increase the detectability of kissing bonds at adherend–adhesive interfaces. This technique interrogates the crucial adherend–adhesive interface only, but it is insensitive to the cohesive properties of the adhesive. This is partly necessary because of inherent inhomogeneities in the adhesive and partly inevitable because of its high ultrasonic attenuation. Consequently, both adherend–adhesive interfaces must be inspected separately. It was shown that the suggested technique can detect very weak kissing-bond defects entirely hidden from conventional ultrasonic inspection.

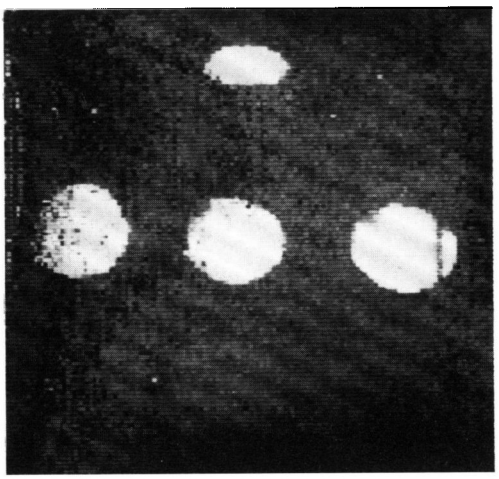

Figure 13. Conventional 10 MHz normal incidence C-scan of kissing bonds turned into gross delaminations by bending.

Acknowledgements

I wish to thank L. Adler, R. Ko, and W. Sheppard for their valuable contributions. This work was sponsored by the Northrop Corporation.

REFERENCES

1. J. P. Jones and J. S. Whittier, *J. Appl. Mech.* **34**, 905 (1967).
2. H. G. Tattersall, *J. Phys.* **6**, 819 (1973).
3. M. Schoenberg, *J. Acoust. Soc. Am.* **68**, 1516 (1980).
4. J. M. Baik and R. B. Thompson, *J. Nondestr. Eval.* **4**, 177 (1984).
5. R. B. Thompson and C. J. Fiedler, in: *Review of Progress in Quantitative NDE*. D. O. Thompson and D. E. Chimenti (Eds), Vol. 3A, pp. 207–215. Plenum Press, New York (1984).
6. Y. C. Angel and J. D. Achenbach, *J. Appl. Mech.* **107**, 33 (1985).
7. Y. C. Angel and J. D. Achenbach, in: *Review of Progress in Quantitative NDE*. D. O. Thompson and D. E. Chimenti (Eds), Vol. 4A, pp. 83–89. Plenum Press, New York (1985).
8. A. Pilarski and J. L. Rose, *J. Appl. Phys.* **63**, 300 (1988).
9. F. J. Margetan, R. B. Thompson and T. A. Gray, *J. Nondestr. Eval.* **7**, 131 (1988).
10. Y. C. Angel and J. D. Achenbach, *Wave Motion* **7**, 375 (1985).
11. D. A. Sotiropoulos and J. D. Achenbach, *J. Acoust. Soc. Am.* **84**, 752 (1988).
12. D. A. Sotiropoulos and J. D. Achenbach, *J. Nondestr. Eval.* **7**, 123 (1988).
13. H. Tada, P. Paris and G. Irwin, *The Stress Analysis of Cracks Handbook*. Del Research, St. Louis, MO (1973).
14. N. F. Haines, *The Theory of Sound Transmission and Reflection at Contacting Surfaces*, RD-B-N4744. Berkeley Nuclear Laboratories (1980).
15. P. B. Nagy and L. Adler, *J. Nondestr. Eval.* **7**, 199 (1988).
16. S. I. Rokhlin and D. Marom, *J. Acoust. Soc. Am.* **80**, 585 (1986).
17. P. B. Nagy, L. Adler and W. Sheppard, in: *NDE of Advanced Bonds and Bondlines*, pp. 62–73. ASNT, Columbus (1989).